IT 10 054
Examensarbete 30 hp
Oktober 2010

Optical Properties of Materials Calculated from First Principles Theory

Raghuveer Chimata

Institutionen för informationsteknologi
Department of Information Technology

To my teacher Biplab Sanyal

UPPSALA
UNIVERSITET

Teknisk- naturvetenskaplig fakultet
UTH-enheten

Besöksadress:
Ångströmlaboratoriet
Lägerhyddsvägen 1
Hus 4, Plan 0

Postadress:
Box 536
751 21 Uppsala

Telefon:
018 – 471 30 03

Telefax:
018 – 471 30 00

Hemsida:
http://www.teknat.uu.se/student

Abstract

Optical Properties of Materials Calculated from First Principles Theory

Raghuveer Chimata

In this project work, we performed ab-inito calculations for 20 different non-magnetic materials (band gap ranging between 0.5 eV to 13 eV) and three different magnetic materials such as NiO, EuO and GdN using density functional theory (DFT). Generalized gradient approximation (PBE) and hybrid functional (HSE06, PBE0) within projector-augmented wave (PAW) methodology were adopted to investigate the electronic properties, whereas only PBE approximation was used to study optical properties of these materials. Furthermore, for magnetic materials, PBE+U method was employed to treat the strongly correlated d and f electrons. Subtle difference in f electron state at the Fermi level in EuO and GdN for different approximations was thoroughly evaluated here. Using HSE06 we have showed that for non-magnetic materials the band-gap values were comparable with the experimental values. For EuO we have observed a band-gap of 0.8 eV by using PBE+U approximation. However, in the HSE06 approximation, no band-gap was observed at Fermi level. The optical properties for non-magnetic systems were evaluated by calculating the dynamic dielectric functions such as absorption, reflection and energy-loss spectroscopy with the help of self-developed numerical codes. The static dielectric matrices of materials were calculated using density functional perturbation theory. The static dielectric constant values were calculated by different approaches: i) by including local field effects in both DFT and random phase approximations (RPA) and ii) excluding local field effects and including local field effects in DFT. The static constant values of the materials including local field effects for RPA approximation yielded better results than other methods.

Handledare: Biplab Sanyal
Ämnesgranskare: Lars Nordström
Examinator: Anders Jansson
IT 10 054
Tryckt av: Reprocentralen ITC

Contents

Chapter 1

Introduction

Use of simulation and modelling techniques help to design semiconducting materials at a macroscopic level, which represents equations those define the macroscopic material properties in terms of parameters (mass, diffusion coefficient etc), which fits with the experimental results. Today, the increasing application of computation techniques have made these approaches more realistic at microscopic level (e.g. diffusion barrier) and also electronic states can be explained in a better way. These computational techniques allowing direct applications of ab-initio quantum calculation to realistic systems. Much work are needed to be done in these fields, which might allow engineers to understand the physical properties of elementary components. However the theoretical calculations in these materials are not trivial.

These bulky semiconducting materials obey quantum mechanics and they are truly many body problems. Density functional theory (DFT) is an extremely successful approach used to solve many body problems and to calculate the first principles electronic structure. In 1964, Hohenberg and Kohn made conceptual roots to this theory (2).

Local density approximation (LDA) is one of the first exchange-correlation functional, which uses local density of a charge to evaluate the exact functional within that density, later this LDA approximation was modified by introducing the up and down electron spins know as local spin-density approximation (LSDA) (4). Further, by including the gradient of density in LSDA approximation a new functional was framed know as generalized gradient approximation (5)(6)(7).

In this present work, we have studied the electronic structure and optical properties of non-magnetic and magnetic materials. PBE, PBE+U, PBE0 and HSE06 expand all these terms functional were used to calculate the electronic and band

structure calculations within PAW methodology. PBE0 hybrid functional uses 25% of the exchange and 75% PBE exchange and 100% of PBE correlation energy (8). However, HSE06 screened coulomb hybrid density functional uses a short range Hartree-Fock exchange to produce exchange energies from traditional hybrids.

These hybrid functional were used to study d and f electronic systems such as NiO, MnO, EuO and GdN. The f electron systems are of particular interest because they possess f density of states near fermi level and it makes more difficult to know exact exchange of the electrons.Studying the microscopic polarizability matrix of frequency dependent dielectric function is important to interpret the optical properties of materials.Adler and Wiser derived the functions for a periodic systems (10)(11). The frequency dependent dielectric matrices were calculated using summation over conduction band method after obtaining the self consistent Eigen values from PBE approximations. Similarly static dielectric function calculated from density functional perturbation theory within linear response theory, by summation over empty bands. However, the static dielectric function was calculated excluding the local field effects and including local effects within random phase approximations (RPA) and DFT levels (12). Macroscopic electric field effects and induced dipole moments from near site atoms causes local field effects.In random phase approximation, the electrons were respond to sum of external macroscopic field and screening potential(9).

The thesis is organized as follows: In chapter 2 we described theoretical background of many body problems. In chapter 3 we describe the computational methods used in our thesis work. In chapter 4 we presented DOS and band structure calculations for the materials and compared with other theoretical works. In last chapter we discussed about theoretical optical properties of the materials.

Chapter 2

Theoretical background

In this chapter we introduce the many-body quantum mechanics problem in first section.In second section we present the Born-Oppenheimer approximation to solve many-body Hamiltonian by considering the kinetic energy of nuclei as zero , the new Hamiltonian consists of motion of electrons lonely in a constant potential. In third section we discussed evolution of DFT theory and success of it. In later sections we discussed about different approximations to solve for exact-exchange functionals by taking charge density as a basic variable. In final section Bloch electrons and plane wave method are explained.

2.1 The many-body problem

The main task in computational material science is to solve the electronic structure of atoms, molecules and bulk materials. Atoms are made up of electrons and nuclei. In quantum mechanics, the electron is considered as wave functions rather than a classical particle. The solid or quantum system exhibits different electronic, electrical, transport and optical properties. Schordinger equation is used to solve the electronic structurel of any time independent quantum system. The equation is given below

$$\hat{H}\Psi = E\Psi \tag{2.1}$$

where,

$$\begin{aligned} \hat{H} &= -\frac{\hbar^2}{2m_e}\sum_i \nabla_i^2 - \sum_{i,I}\frac{Z_I e^2}{\mid r_i - R_i \mid} + \frac{1}{2}\sum_{i\neq j}\frac{e^2}{\mid r_i - r_j \mid} \\ &- \sum_I \frac{\hbar^2}{2M_I}\nabla_I^2 + \frac{1}{2}\sum_{I\neq J}\frac{Z_I Z_J e^2}{\mid R_I - R_J \mid} \end{aligned} \tag{2.2}$$

where m_e and M_I represent the electron mass and nuclei mass respectively, r_i and R_I are positions of electron and nuclei. Z_I is charge of nuclei and e is charge of electron. The complex system is made-up of electrons and nuclei interacting each other due to coulomb force. The first term and fourth term represent the kinetic energy of electrons and nuclei respectively, second term is the attractive interaction between the electron and nuclei, third term is electron-electron repulsion term,the last term is nuclei-nuclei repulsion. Since the real Hamiltonian of solids consists of electrons and nuclei of the order of 10^{23} the problem is impossible to solve. So we need new approximations to solve the many-body problem.

2.2 Born-Oppenheimer approximation

Born-Oppenheimer approximation is the early approximation used to solve the Hamiltonian by considering the fact that the nuclei can not move as much as electron due to its heavy mass, thus, the kinetic energy of nuclei term was omitted from the Hamiltonian equation and new Hamiltonian is given by (1)

$$\hat{H} = -\frac{\hbar^2}{2m_e}\sum_i \nabla_i^2 + \frac{1}{2}\sum_{i\neq j}\frac{e^2}{\mid r_i - r_i \mid} + V_{R_\alpha}^{ext}(r_i) \tag{2.3}$$

Even after omitting the nuclei terms in old Hamiltonian still the electrons is in the order of 10^{23} making a exact solution impossible. Therefore, a new approximation is necessary, to solve the hamiltonian whereby considering number of independent particles (electrons) or by other variables as input.

2.3 Density Functional Theory(DFT)

Density functional theory is the most successful method that forms the basis for advanced ab-inito calculations. By using DFT theory it is possible to calculate the properties of solids and molecules. The DFT uses as a basic variable the electron density rather than considering many interacting and non-interacting electron wave functions in the external potential. DFT was formerly framed on basic two theorems.

2.3.1 The Hohenberg-Kohn theorems

2.3.1.1 Theorem 1:

The Hohenberg-Kohn theorem 1 states that if there are N interacting particles in a system and they are moving in an external field $V_{ext}(r)$, the $V_{ext}(r)$ is uniquely determined by the ground state particle density $n_0(r)$, except a constant, that

mean there no two potentials exist to give rise to the same ground state, except a constant.(13)

The ground state expectation value of any observable(hamiltonaian) is an unique functional of the exact ground-state electron density $\rho_0(r)$

$$\langle \psi \mid A \mid \psi \rangle = A[\rho_0(r)] \tag{2.4}$$

2.3.1.2 Theorem 2:

The second theorem of HK states that a universal functional for energy can be defined in terms of density, which is valid for any applied external potenial. The functional of the exact ground state energy of a system that will have lowest energy only when the input density is the real ground density state(13).

$$E_0 \leq E[\tilde{\rho}] = T[\tilde{\rho}] + E_{Ne}[\tilde{\rho}] + E_{ee}[\tilde{\rho}] \tag{2.5}$$

From the above first theorem one can conclude that if we know the ground-state particle density, it is possible to reconstruct the new hamiltonian. Schrodinger equation was used to solve the new many-body wave functions for new $\hat{H}$. They are independent of number of particles and purely dependent on electron density. The Second theorem states that the exact ground state is the global minimum value of the functional.

2.3.2 Kohn-Sham approximation

Kohn-Sham proposed new approach to solve many electron system based on the H-K theorems[15]. Total energy functional in an external potential $V_{ext}(\vec{r})$can be

$$E[\rho(\vec{r})] = T[\rho(\vec{r})] + \int V_{ext}(\vec{r})\rho(\vec{r})d^3r + E_{ee}[\rho(\vec{r})] \tag{2.6}$$

$$E_{ee}[\rho(\vec{r})] = \int\int \frac{\rho(\vec{r})\rho(\acute{r})}{\mid r - \acute{r} \mid} d^3r d^3\acute{r} + \hat{E}_{xc}[\rho(\vec{r})] \tag{2.7}$$

The first term is the kinetic energy $T[\rho(\vec{r})]$, second term is electron-electron potential and last term is contributes both classical and non-classical exchange behind the mean field theory. To solve the Kohn and Sham equations it is assumed that for an interacting system describing the equation, there is a reference non-interacting system with ground state density same as interacting system. The equation for the reference system can be written as

$$H_{eff} \mid \psi_i\rangle = [-\sum_i \nabla_i^2 + V_{eff}[\rho(\vec{r})] \mid \psi_i\rangle = \varepsilon_i \mid \psi_i\rangle \tag{2.8}$$

Then we have a kinetic energy of this system is

$$T_{eff}[\rho(\vec{r})] = \sum_i n_i \varepsilon i - V_{eff}[\rho(\vec{r})] \tag{2.9}$$

The new pseudo kinetic energy in the form of exchange correlation energy functional $E_{xc}[\rho(\vec{r})]$ as

$$E_{xc}[\rho(\vec{r})] = T[\rho(\vec{r})] - T_{eff}[\rho(\vec{r})] + \hat{E_{xc}}[\rho(\vec{r})] \tag{2.10}$$

By inserting the new exchange correlation functional into total energy system and there by deriving the new total energy of the non-interacting system which is in effective potential with respect to $\rho(\vec{r})$ by conserving the density, $\int \rho(\vec{r})dr = N$, where N is the total number of electrons.

By solving the above equation 11 and equation 12 we get

We will obtain final Kohn-Sham equation by solving the one-electron Schrodinger-like equation which is moving in a potential V_{eff} is

$$\left[-\nabla^2 + V_{eff}[\rho(\vec{r})]\right] \psi_i(\vec{r}) = \varepsilon_i \psi_i(\vec{r}) \tag{2.11}$$

and we got final ground state energy is

$$E_0 = \sum_i n_i \varepsilon_i - \int\int \frac{2\rho(\acute{r})}{\mid r - \acute{r} \mid} d^3\acute{r} - \int \frac{\delta E_{xc}[\rho]}{\delta \rho(\vec{r})} d^3r + E_{xc}[\rho(\vec{r})] \tag{2.12}$$

Where E_{xc} is the exchange-correlation potential with unknown knowledge till. So if we know the exact functional of E_{xc} then we know the exact solution of the many electron system. In coming section we will discuss the Exchange-correlation functional in detail.

2.3.3 Self-consistent Kohn-Sham equation

Here,we disscuss self-consitent Kohn-Sham algorithm to calcaulte ground state density and its energy from the Kohn-Sham noninterating system equation.In first step, we assumed some initial electron density and with that one we calculat the effective potential energies and pass in K-S equations to calcualte new electron density. The diagonalization of Hamiltonian in K-S equations can be done by using different diagonolization methods. The new electron density from previous step is compared with old density. If the difference of two electron densties is zero

then we stop the calculation otherwise put the new electron density into first step and repeat the above steps upto converged solution. Converged electron density is used to calculate the eigenvalues, forces, energies and stresses.

2.3.4 Exchange-Correlation functional approximations

The Kohn-Sham equations are unsolved till. No analytical solution has been made yet, so we need more approximations to solve this puzzle.The new approximations such as Local Density Approximation(LDA), Generalised Gradient Approximations are implemented analytically and they solved many puzzles of DFT.

2.3.4.1 LDA

The Local Density Approximation is an approximation for the exchange-correlation(xc), which can be defiend as

$$E_{xc}^{LDA} = \int d^3r \varepsilon_{xc}(n_0) \mid_{n_0 \to n(r)} \tag{2.13}$$

where $\varepsilon_{xc}(n_0) \mid_{n_0 \to n(r)}$ is the exchange-correlation energy in a homogeneous electron gas with the density $n_0 = n(r)$,i,e., replacing the with local density $n(r)$ of an inhomogeneous system at each point r by the constant density n_0 of homogeneous electron gas.(4)

In Local spin Density Approximation(LSDA) exchange-correlation functional can be obtained by introducing the spin-resolved densities as $\rho(r) = \rho_\uparrow(r) + \rho_\downarrow(r)$ and the new exchange-correlation for magnetic materials can be defiend as

$$E_{xc}^{LSDA}[\rho_\uparrow(r), \rho_\downarrow(r)] = \int [\rho_\uparrow + \rho_\downarrow] \varepsilon_{xc}^{hom}[\rho_\uparrow, \rho_\downarrow] dr \tag{2.14}$$

In reality the density is expressed in the form of a dimension less quantity r_s which is the radius of the sphere known as Wigner-Seitz radius, which is an average orbital of an electron. Dirac deduced the exchange energy density is(14)

$$\varepsilon_x[\rho] = -\frac{3}{4}\left(\frac{3}{\pi}\right)^{\frac{1}{3}} \rho^{\frac{1}{3}} = -\frac{3}{4}\left(\frac{9}{4\pi^2}\right)^{\frac{1}{3}} \frac{1}{r_s} = -\frac{0.458}{r_s} au \tag{2.15}$$

We expressed the exchange energy in above formula and now we need the correlation energy. The correlation energy approximation is parametrized in Perdew and Zungers paper.

The correlation energy is widely explained in Perdew and Zunger's paper(15).Ceperley and Alder(16) parametrized the correlation energy for high density $r_s \geq 1$ and low density $r_s < 1$ by using Monte carlo methods.

In high density limit $r_s \geq 1$, the kientic energy dominates and in low density limit $r_s < 1$ the electrostatic force dominates. But in real materials the r_s is of the order of unity.

2.3.4.2 GGA

LDA approximation fails to predict exact exchange energy when its density undergoes rapid changes, in molecules(17).This problem can be solved by considering the gradient of the electron density. The GGA approximation principally made by Perdew and co-workers(5)(6)(7).

The exchange-correlation energy is defined as,

$$E_{xc} = E_{xc}[\rho(r), \nabla\rho(r)]] \tag{2.16}$$

2.3.4.3 PBE

PBE is a new version of GGA. The exchange energy of PBE approximation can be defined as an integral over the exchange density (20).

$$E_x^{PBE} = \int dr\rho(r)\varepsilon_x^{PBE}(\rho(r), s(r)) \tag{2.17}$$

where $s = \mid \nabla \mid /(2k_F\rho)$ is the reduced gradient with $k_F = (3\pi^2\rho)^{\frac{1}{3}}$.

The PBE exchange energy density is the product of LDA exchange and enhancement factor, F_x^{PBE} which depends on $s(r)$, which is defined in explicitly PBE functional.

$$\varepsilon_x^{PBE}(\rho(r), s(r)) = \varepsilon_x^{LDA}(\rho(r)) \times F_x^{PBE}(s(r)) \tag{2.18}$$

$$F_x^{PBE}(s) = -\frac{8}{9}\int_0^\infty ydyJ^{PBE}(s, y) \tag{2.19}$$

where $J^{PBE}(s, y)$ is the PBE exchange hole

2.4 Bloch electrons and plane wave method

For solids, the wave function of an electron placed in a periodic potential i.e., the effective potential derived in K-S equation has a periodicity of the cystalline lattice. From Bloch's theorem we can write K-S orbitals,$\psi_k^n(r)$, as a product of a plane wave $e^{ik.r}$ and periodic function, $u_k^n(r)$ that has periodicity of the lattice.

$$\psi_k^i(r) = u_k^n(r)e^{ik.r} \tag{2.20}$$

where k is vector in first Brillouin zone and n is a band index.
Due to its periodicity $u_k^n(r)$ can be expanded as a set of plane waves

$$\psi_k^n(r) = \frac{1}{\sqrt{\Omega_{cell}}} \sum_j c_j^n(k) e^{i(k+k_j)\cdot r} \tag{2.21}$$

where k_j is the reciprocal lattice vector,Ω_{cell} is the volume of the primitive cell. Transferring the K-S orbitals to plane wave basis set, we obtained

$$\sum_{j'} H_{j,j'}(k) c_{j'}^n(k) = \varepsilon_n(k) c_j^n(k) \tag{2.22}$$

where

$$H_{j,j'}(k) = \frac{\hbar^2}{2m} \mid k + K_j \mid \delta_{j,j'} + V_{eff}(K_j - K_{j'}) \tag{2.23}$$

The above term is the matrix element of kinetic energy operator where the plane waves are orthonormalized once. and

$$V_{eff}(K_j - K_{j'}) = \int_{\Omega_{cell}} V_{eff}(r) e^{i(k_j - k_{j'})\cdot r} \tag{2.24}$$

Where k and K are real space wave and reciprocal lattice vectors respectively. The above term is effective potential. By diagonalization of Hamiltonian are, can get discrete set of eigenvalues and corresponding eigenfunctions for all n band index at each k-point. The energy eigenvalue looks like,

$$\varepsilon_n(k) = \varepsilon_n(k + K) \tag{2.25}$$

We can choose cut-off vector in reciprocal space, $\mathbf{K}$ as $K \leq K_{max}$, where K_{max} is the reciprocal space wave vector corresponding to the energy cut-off.

2.5 Projector augmented wave(PAW) method

It is important to know features of wave functions because at the nuclei region the waves functions oscillate rapidly and at delocalized region they are smooth in nature. Calculations of these wave functions are necessary. To get augmented wave methods the wave functions are divided into two parts, first part of partial waves are expanded within an atom-centered region and second part is expanded near envelope region called as envelope functions.In this section one of augmented wave function know as PAW is going to be explained here (19).

PAW is a general method for all-electron solution has been developed by Blochl(19).The PAW has been made up by combining the features of plane-wave

pseudo potential method and linear augmented plave wave(LAPW) method. In PAW method, the pseudo-wave-functions $|\tilde{\psi_n}\rangle$ are linearly transformed to get one electron wave functions $|\psi_n\rangle$

$$|\ \psi_n\rangle = |\ \tilde{\psi_n}\rangle + \sum \left(|\ \phi_i\rangle - |\ \tilde{\phi_i}\rangle \right) \langle \tilde{\mathbf{p}}_i \mid \tilde{\psi_n}\rangle \tag{2.26}$$

The relation is made up on definition of augmentation volume, Ω_R, where R is the atomic site, in which the partial waves $|\ \phi_i\rangle$ form a basis of atomic wave functions, where $\tilde{\mathbf{p}}_i$ is are set of projectors on partial waves $|\ \tilde{\phi_i}\rangle$.

2.6 Hybrid functionals

2.6.1 A screened Coulomb potential hybrid functional

We have severe problems in GGA,LDA and PBE functionals. In these functions d and f electrons cannot be treated properly due to insufficient electron correlations and relativistic effects. To overcome these problems we propose new hybrid functionals which make the exact exchange mixing within short range interaction within the HF and DFT levels.

Here we propose new hybrid functional, which uses PBE exchange-correlation functional. The new hybrid scheme can be expressed in linear expression by using a mixing coefficient a=1/4 obtained from perturbation theory(21).

$$E_{xc}^{PBE0} = aE_x^{HF} + (1-a)E_x^{PBE} + E_c^{PBE} \tag{2.27}$$

Where E_{xc}^{PBE0} is PBE exchange-correlation, E_x^{PBE} is PBE exchange part, E_c^{PBE} is PBE correlation part E_x^{HF} is the HF exchange. The PBE0 exchange functional is important to consider and can be written as

$$E_x^{PBE0} = aE_x^{HF} + (1-a)E_x^{PBE} \tag{2.28}$$

Further each component of exchange functional is divide into short range and long range terms

$$\begin{aligned} E_x^{PBE0} &= aE_x^{HF,SR}(\omega) + aE_x^{HF,LR}(\omega) \\ &+ (1-a)E_x^{PBE,SR}(\omega) + E_x^{PBE,LR}(\omega) - aE_x^{PBE,LR}(\omega) \end{aligned} \tag{2.29}$$

Using Hartree-Fock screaning parameter $\omega = 0.15$ the long range PBE and HF exchange contributions cancele each other and we get a new hydrid functional known as Heyd, Scuseria and Ernzerhof(HSE) functional and the new hybrid functional can be written as(22)(23)(24).

$$E_{xc}^{HSE} = aE_x^{HF,SR}(\omega) + (1-a)E_x^{PBE,SR} + E_x^{PBE,LR}(\omega) + E_c^{PBE} \tag{2.30}$$

2.7 Optical Properties

The optical processes such as absorption, reflection and transmission are observed in solids. These processes can be quantified by a number of parameters in the solids. The parameters can described by the properties of solids at microscopic and macroscopic levels. In this section, we present the optical processes at a microscopic level. At microscopic or quantum mechanical level in bulk solids the complex dielectric function is closely connected with the band structure. The expresion for the complex imaginary dielectric function $\varepsilon_2(\omega)$ has been derived in PAW methodology by summing over conduction bands (25),

$$\varepsilon^{(2)}_{\alpha\beta}(\omega) = \frac{4\Pi^2 e^2}{\Omega}\frac{1}{q^2}\lim_{q\to 0}\sum_{c,v,k} 2w_k\delta(\epsilon_{ck}-\epsilon_{vk}-\omega)\times\langle u_{ck+e_\alpha q}|u_{vk}\rangle\langle u_{ck+e_\alpha q}|u_{vk}\rangle^* \quad (2.31)$$

In the above equation the transitions are made from occupied to unoccupied states within the first Brillouin zone, the wave vectors are fixed **k**.Real and Imaginary parts of analytical dielectric function are connected by the Kramers-Kronig relation as,

$$\varepsilon^{(1)}_{\alpha\beta}(\omega) = 1 + \frac{2}{\Pi}\mathbf{P}\int_0^\infty \frac{\varepsilon^{(2)}_{\alpha\beta}(\omega')\omega'}{\omega'^2-\omega^2+i\eta}d\omega' \quad (2.32)$$

The reflectivity equation is given by,

$$R(\omega) = \left|\frac{\sqrt{\varepsilon(\omega)}-1}{\sqrt{\varepsilon(\omega)}+1}\right|^2 \quad (2.33)$$

The Energy-loss spectrum, Refractive index and extinction coefficient formulae are presented below.

$$L(\omega) = \frac{\varepsilon_2(\omega)}{\varepsilon_1^2(\omega)+\varepsilon_2^2(\omega)} \quad (2.34)$$

$$n = \left[\frac{\sqrt{\varepsilon_1^2+\varepsilon_2^2}+\varepsilon_1}{2}\right]^{\frac{1}{2}} \quad (2.35)$$

$$k = \left[\frac{\sqrt{\varepsilon_1^2+\varepsilon_2^2}-\varepsilon_1}{2}\right]^{\frac{1}{2}} \quad (2.36)$$

.

2.7.1 Static dielectric constant

During the last decade, theoretical calculations of local effects on the static dielectric constant were implemented in different ab inito codes. In linear response theory the system is subjected to small perturbation, the relation between the external potential from the perturbation and the total potential is given by the inverse of the static dielectric function in a reciprocal space a ε^{-1}. The general expression in the perturbation theory as(25)

$$\mid \nabla_{\mathbf{k}} \tilde{u}_{n\mathbf{k}} \rangle = \sum_{n' \neq n} \frac{|\tilde{u}_{n'\mathbf{k}}\rangle \left\langle \tilde{u}_{n'\mathbf{k}} \left| \frac{\partial[\mathbf{H}(\mathbf{k}) - \varepsilon_{n\mathbf{k}} \mathbf{S}(\mathbf{k})]}{\partial \mathbf{k}} \right| \tilde{u}_{n\mathbf{k}} \right\rangle}{\varepsilon_{n\mathbf{k}} - \varepsilon_{n'\mathbf{k}}} \tag{2.37}$$

The variation in DFPT can be determined by Sternheimer equation linearly is(26)

$$(\mathbf{H}(\mathbf{k}) - \varepsilon_{n\mathbf{k}} \mathbf{S}(\mathbf{k})) \mid \nabla_{\mathbf{k}} \tilde{u}_{n\mathbf{k}} \rangle = -\frac{\partial(\mathbf{H}(\mathbf{k})) - \varepsilon_{n\mathbf{k}} \mathbf{S}(\mathbf{k}))}{\partial \mathbf{k}} \mid \tilde{u}_{n\mathbf{k}} \rangle \tag{2.38}$$

2.7.2 Direct Interband Transition

The transition probability is made between eletrons and photons only at the same k point of valence and conduction bands.

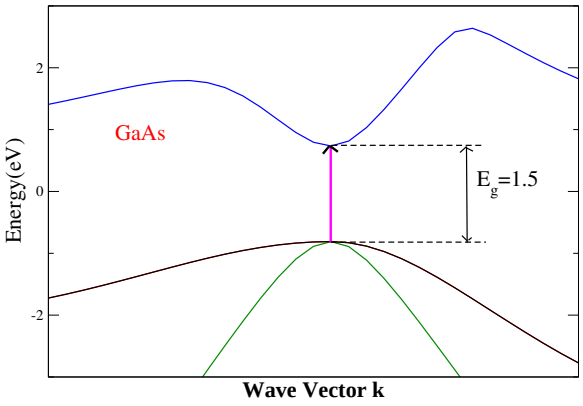

Figure 2.1: Direct band transition

2.7.3 Indirect Interband Transition

This transition probability is made between the electrons and photons by considering vibrations of an crystal.

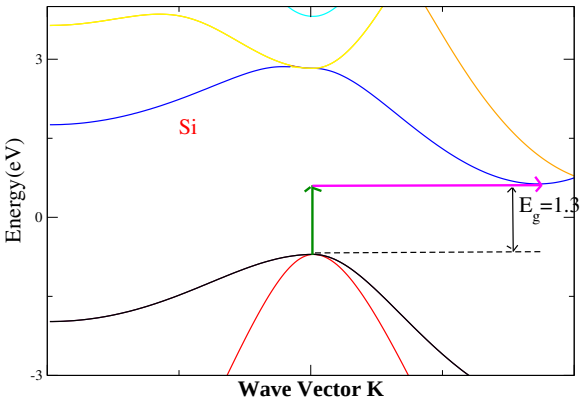

Figure 2.2: Indirect band transition

Chapter 3

Computational details

In this section DFT approximations to calculate the DOS and band-structures have been described. In the second part we discuss about optical properties.

3.1 PBE and HSE functionals

In this work, group III-IV, GaAs, InP,InSb and group IV semiconductors , Si, Ge are zinc-blende structures and C has diamond structure, group ZnO and GaN are wurzite structure were used in this thesis. The electronic structure calculations were performed with VASP5.2 programs within PAW methodology. We used 9x9x9 Monkhorst k-point mesh. The lattice parameters of above materials are shown in table [4.1]. In HSE calculations Monkhorst k-point sample mesh were used .All ionic relaxation were performed with a tolerance of 0.00001 eV. We applied tetrahedron method to compute DOS calculations in PBE and HSE calculations. Band structure calculations were performed in non-selfconsistent way by using 400 kpoints for most of the materials.

3.2 Optical Calculations

The frequency dependent dielectric matrix was calculated using VASP 5.2 optical programs. The calculations were carried out in longitudinal by increasing the conduction bands by three times. All the calculations were performed using 9x9x9 grid mesh of Monkhorst-pack scheme. Imaginary dielectric and real dielectric values of materials were plotted for all photon energies. The reflection, energy-loss spectrum, refractive index were calculated using formulas 2.33, 2.34, and 2.35 respectively by using real and imaginary parts of dielectric function. A FORTRAN program was coded to get these properties presented in appendix[1]. The important optical transition peaks are shown in dielectric imaginary plots.

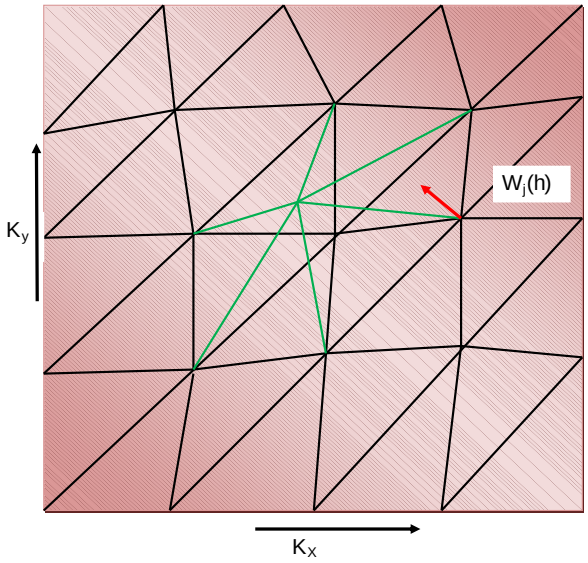

Figure 3.1: Tetrahedron integration along Kx and Ky vectors

In static dielectric calculation,the number of empty bands were kept constant for all the calcaultions.

3.3 Numerical Methods in VASP

In this section I am presenting smearing methods which I used in this work.

3.3.1 Tetrahedron method with Blochl corrections

For performing Brillouin-Zone(BZ) integration we used tetrahedron method in this work. In this method, the reciprocal space is divided into tetrahedra as shown in figure 3.1. Each corner of a tetrahedron can be represented by k-point of BZ and eigenvalues can be obtained for each k-point.The matrix elements and eigenvalues can be linearly interpolated and to be intergrated X_n within tetrahedra. The intergration running over all tetrahedron can be written as,

$$\bar{X_n} = \sum_j c_j X_n(\mathbf{k}_j) \tag{3.1}$$

The tradiational tetrahedron integration method has some drawbacks. It may break the symmetry of the Bravais lattice and it uses four k-points at least to form a tetrahedron, within four k-points there is a gamma point.While computing

the interpolation analytically it may be over or under estimated and these errors were rectified by Blochl (19).

3.3.1.1 Davidson block iteration scheme

The K-S equation expanded in projector augmented wave method has been characterized by a set of expansion coefficients and n is the number of eigenstates. The simple generalized eigenvalue of Hamiltonian H and overlap matrix S problem can be written as

$$H\phi_n = \varepsilon_n S\phi_n \tag{3.2}$$

The above eigenvalue problem is solved by diagonalizing of the Hamiltonian. Solving the Large Hamiltonian matrices is a big deal. To diagonalize the large matrices we need iterative methods. One such iterative method which was implemented in vasp5.2 version is Block-Davidson method. Originally the method was implemented by Davidson and Liu by simultaneous updating of the number of bands in each expansion of plane wave basis set. In expansion of plane wave basis step for each iteration it was expanded by N_b ,N_b is the number of bands. In this method, precondition residual vectors were used to update the eigenvectors for each iteration step. Rayleigh-Ritz scheme is used to calculate the eigenvectors. From the new eigenvectors the precondition residual vectors were updated and the iterations were continued up to the solution converged(18).

3.3.2 Platforms

To run Vasp5.2 programs we used Kalkyl and ISIS clusters in UPPMAX. Each node of kalkyl consists of two Quad-core Intel Xeon 5520 processors and ISIS has a dual AMD Opteran, dual core processors in each node. A detailed description of computational hours were given in Table[3.1].

Structure	Cluster type	No of Nodes	No of CPU hours for PBE	No of CPU hours for HSE
Ge	ISIS	1	2 Mins	4 Hours
Si	ISIS	1	2 Mins	4 Hours
ZnO	ISIS	1	20 Mins	1.5 Days
TiO2	ISIS	1	20 MIns	2 Days
NiO	Kalkyl	3	30 Mins	1 Days
EuO	Kalkyl	4	30 Mins	7 Days
GdN	Kalkyl	4	30 Mins	7 Days

Table 3.1: The computational hours used for PBE and HSE functional for different systems

Chapter 4

Results and discussion

In this chapter in first section we compare band gap of group IV: Ge, Si, diamond, group III-V: GaAs, GaSb, InAs, InP, InSb, AlAs, AlN, AlP, zincblende structures, SiC, LiF, Ne, Ar, NiO, MnO, EuO, GdN rocksalt structures, GaN, ZnO, wurizite structure and TiO2 rutile structures obtained from the PBE and HSE06 approximation. After describing the band gaps of different semiconductors, we discuss about d and f electron systems. In third section we present imaginary, real, absorption, reflectivity plot for GaAs, InAs, Si, diamond, InP and ZnO. In last section we analyse the static dielectric constant of different semiconductors, which we discusse in section 1 of chapter results, and then compare the experimental results with previous results.

4.1 Comparison of band gaps for PBE and HSE06 functions

Band-gaps obtained from different materials ranging from 0.5 to 15 eV were computed using PBE and HSE06 approximations. The band-gaps obtained from the materials by using HSE06 approximation showed good agreement with the experimental data, but in some cases the band-gaps were little bit higher then the experimental values. In this work the structural optimizations were not performed within PBE and HSE06 approximation and I used experimental lattice constant which are presented in Table[4.1]. Due to this reason we got little bit higher values then experimental values. ZnO, NiO, EuO and GdN are not property described by PBE. In ZnO system we got band gap values of 0.7 and 2.4 eV for PBE and HSE06 functional and it is less than the experimental value, 3.142 eV. HSE06 functional cannot the problem completily. The magnetic materials NiO,EuO and GdN are discussed thoroughly in next section.

Symbol	Structure	Band-gap Type	Lattice	PBE Band-gap	HSE Band-gap	Reference
Ge	Zincblende	Indirect	5.640	0.50	0.74	0.74
Si	Zincblende	Indirect	5.430	0.60	1.20	1.17
GaAs	Zincblende	Direct	5.650	0.62	1.45	1.43
SiC	Zincblende	Direct	6.835	1.40	2.3	2.146
ZnO	Wurzite	Direct	3.290	0.70	2.40	3.44
GaN	Wurzite	Direct	3.280	2.23	3.34	3.47
ZnS	Zincblende	Direct	5.420	2.00	3.50	3.91
C	Diamond	Indirect	3.570	4.07	5.10	5.40
BN	Zincblende	Direct	3.620	4.60	6.17	6.1-6.4
MgO	Rock salt	Direct	4.130	4.50	5.40	7.8
LiF	Rock salt	Direct	4.030	8.80	10.00	12-14.4
Ar	FCC	Direct	5.260	8.60	9.60	11-13
Ne	FCC	Direct	4.430	11.68	13.43	15-16
AlAs	Zincblende	Indirect	5.660	1.33	2.12	2.23
AlN	Zincblende	Direct	4.360	3.15	4.70	4.68
AlP	Zincblende	Indirect	5.451	1.63	2.23	2.52
InAs	Zincblende	Direct	6.058	0.25	0.45	
InP	Zincblende	Direct	5.868	0.64	1.392	1.35-1.4
TiO2	Rutile	Direct	4.5937	1.68	2.95	0

Table 4.1: The Material, crystal type, type of gap,experimental lattice constant,PBE band gap,HSE06 band gap were compared with experimental values

AlP and AlSb band structures

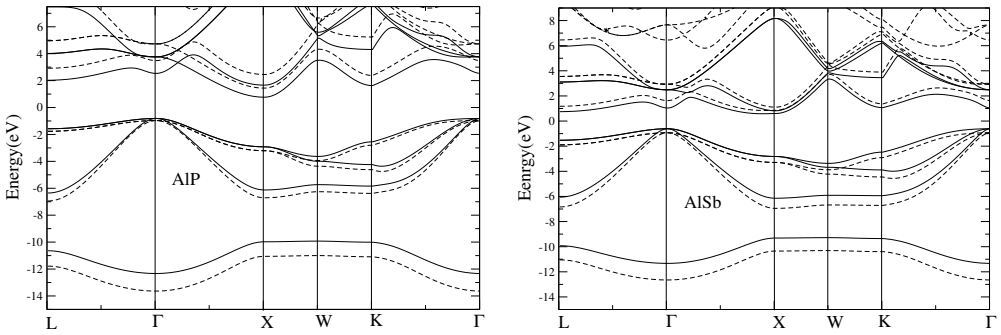

Figure 4.1: The band structure of AlP and AlSb in zinc blende structures are shown here. The solids lines and dashed lines represent PBE and HSE calculations repectively. Calculated HSE band gaps are close to experimental value.

Group IV Ge and Si band strctures

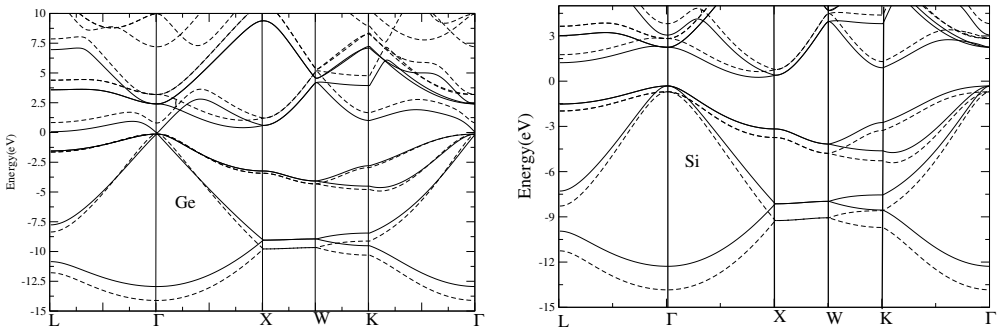

Figure 4.2: The band structure of fourth group Ge and Si in zinc blende structures are shown here. The solids lines and dashed lines represent PBE and HSE calculations repectively. Calculated band-gap of Ge is uncomparable with experimental once. Calculted HSE band gaps for Ge and Si are very close to experimental value.

III-IV GaAs and GaSb band structures

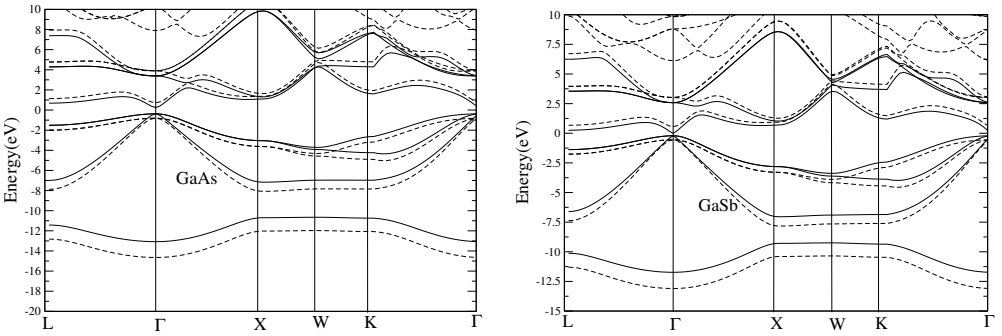

Figure 4.3: The band structure of GaAs and GaSb in zinc blende structures are shown here, the solids lines and dashed lines represent PBE and HSE calculations repectively.

III-IV InP structure

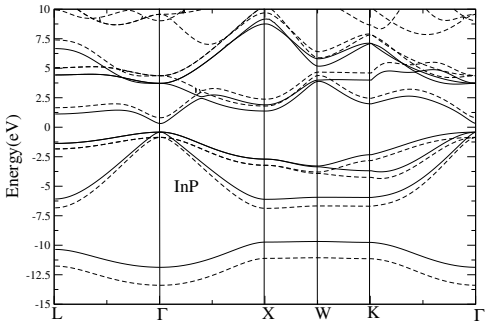

Figure 4.4: The band structure of InP in zinc blende structure is shown here, the solids lines and dashed lines represent PBE and HSE calculations repectively.

Ne and Ar band structures

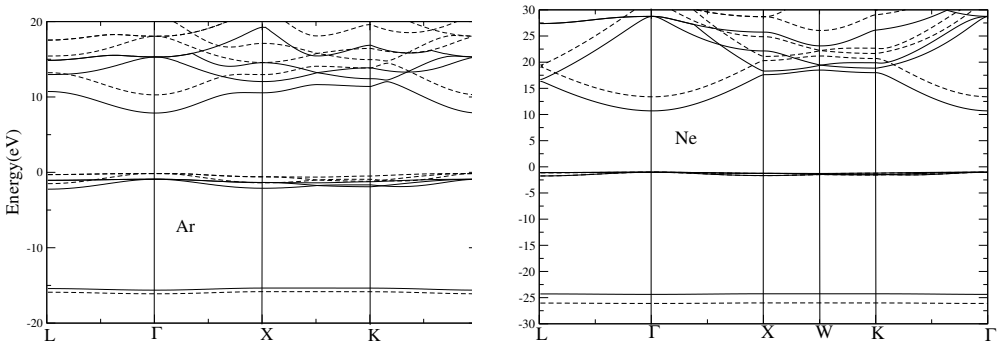

Figure 4.5: The band structure of Ar and Ne structures are shown here, the solids lines and dashed lines represent PBE and HSE calculations repectively.

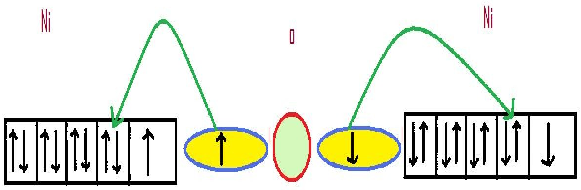

Figure 4.6: Super exchange of NiO AFM II

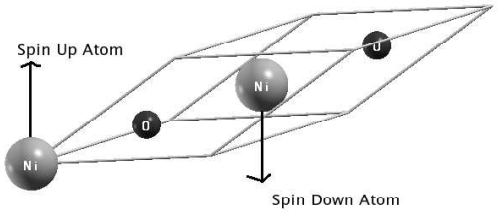

Figure 4.7: Structure of NiO AFM II

4.2 DOS calculations of *d* and *f* electron Systems

NiO is one of intersting oxide systems having d electrons with bad gap of 3.9eV. It crystallizes in NaCl structure. Ni atoms show weak direct exchange interaction J d and strong interaction J s. Where oxgen atoms mediated between two Ni atoms. The exchange interactions were shown in Fig[4.6]. NiO has lowest energy with antiferro II. The primitive unit cell of NiO consists of 2 Ni atoms, 2 Oxygen atoms in its primitive cell and each Ni atom placed at $\langle 111 \rangle$ plane such that magnetic moment of atom in cell cancel each other, it rises antiferro magnetic behaviour, presented in Fig[4.7].

For PBE calculations we obtained a bandgap of 0.7eV. To do PBE+U calculations we used U_d=6 and $J_d = 1.0$ and we got a bandgap of 3.001eV. For HSE06

calculations we obtained a bandgap of 3.3eV. When the bandgap results were compared with experimental bandgap of 4.3 eV it shows that HSE06 cannot fulfill the bandgap.Computed energy difference between the Ferro type and AFM-II structures of NiO has 0.2eV.

After calculated of NiO DOS and Band structure,we got interested in test of f electron systems, we selected EuO, GdN and Gd compounds which exhibits different electronic structure features, having $7f$ electrons which are exactly half-filled in outer shells, has drawn a peculiar interest when compared with whole group of f electron compounds and moreover these materials can be used as spintronic devices. EuO and GdN are f electron magnetic semiconductors and crystallized in rock salt structure like NaCl with lattice constant of and. In europiumoxide Eu has electronic configuration [Xe]$4f^7 5d^0 6s^0$ and that of oxygen has configuration $1s^2 2s^2 2p^6$. EuO has localized magnetic moment of 7.05-7.08 μ_B and has bangap of 1.2eV. Similarly Gadoliniumnitride is one of promising spintronic material with Gd has electronic configuration of [Xe]$4f^7 5d^1 6s^2$, the f electron configuration is very similar to Europium one. Nitrogen has electronic configuration of $2s^2 p^3$. NiO, EuO and GdN has localized magnetic moment of

Symbol	Crsytal Structure	MM(PBE)	MM(PBE+U)	MM(HSE06)	MM(PBE0)
NiO	Rocksalt	0.0	0.0	0.0	0.0
EuO	Rocksalt	7.0	7.0	7.0	7.0
GdN	Rocksalt	7.0	7.0	7.0	7.0

Table 4.2: MM means Bohr magneton, the total magentization were presented

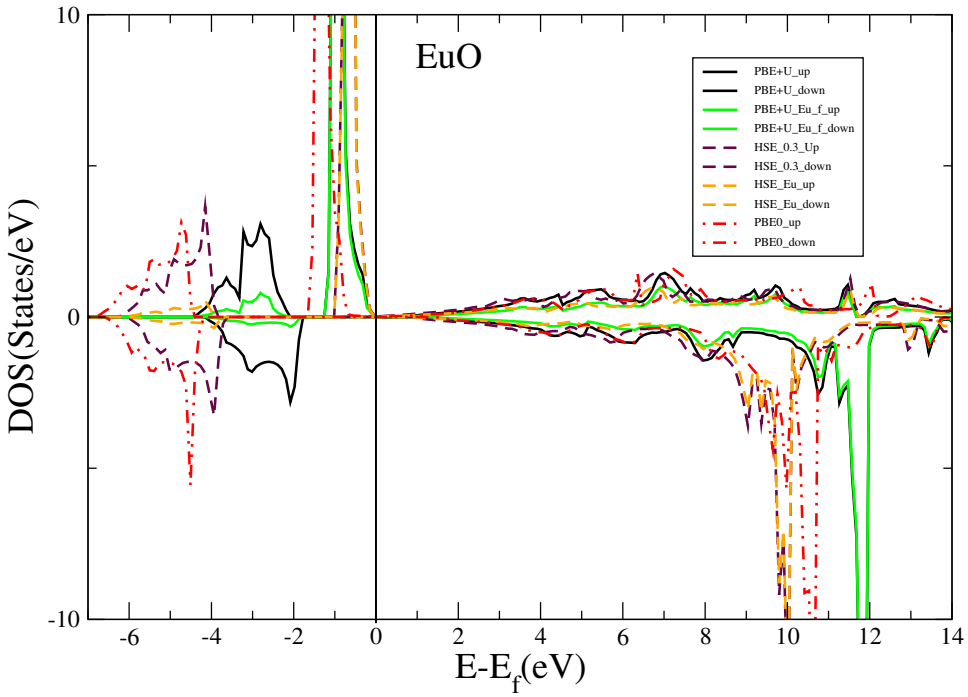

Figure 4.8: Density of states of EuO calculated with different methods are shown. PBE+U opens a gap of 0.9eV and HSE06, PBE0 approximations cannot open a gap.

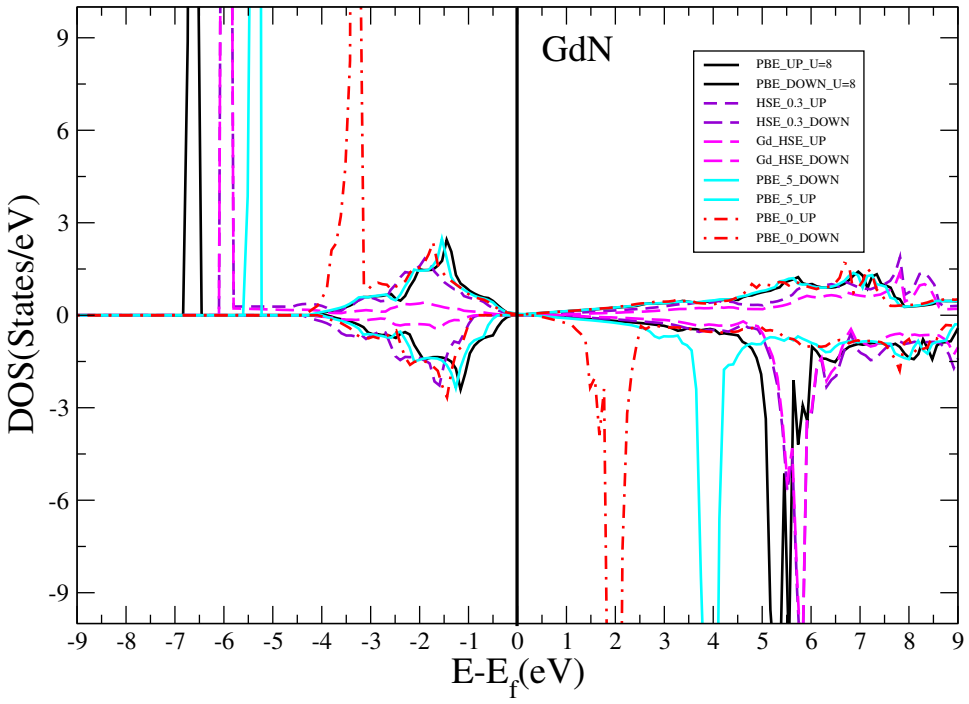

Figure 4.9: Density of states of GdN calculated with different methods are shown.

4.3 Optical Calculations

4.3.1 Dynamic dielectric function

The dynamic dielectric function were discussed within longitudinal expression in optical introduction part. The formulated dielectric function in longitudinal expression in equation [2.31] discussed briefly. After calculating the complex dielectric matrix for all photon energies we computed real, imaginary refractive index ,reflectivity ,absorption and energy loss spectrum. The real part and imaginary parts of complex dielectric function of different semiconductors and insulators are presented in this section.

GaAs Optical plots

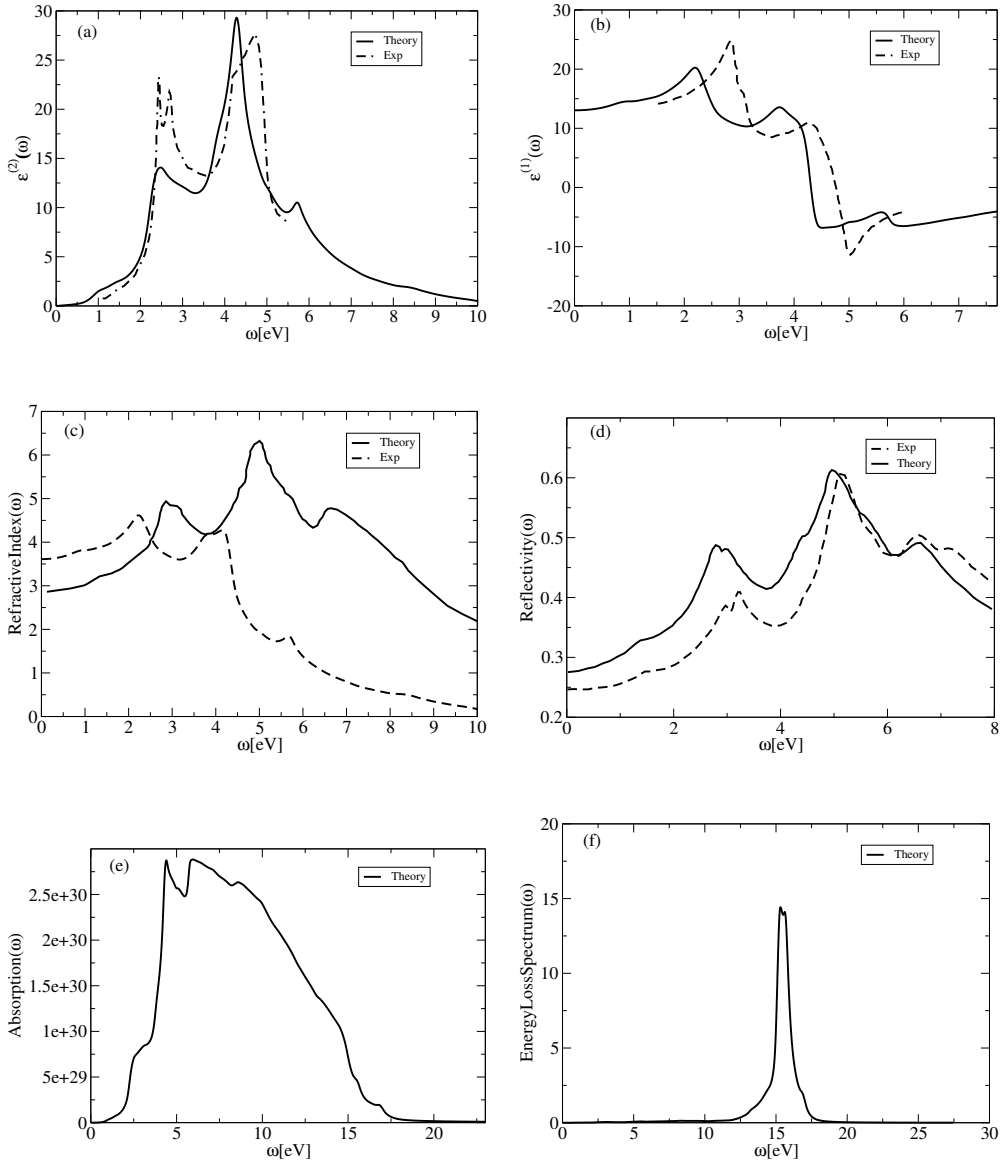

Figure 4.10: Calculated imaginary, real dielectric functions, refractivecoefficient, reflectivity, absorption and EnergylossSpectrum for 3C GaAs

Si Optical plots

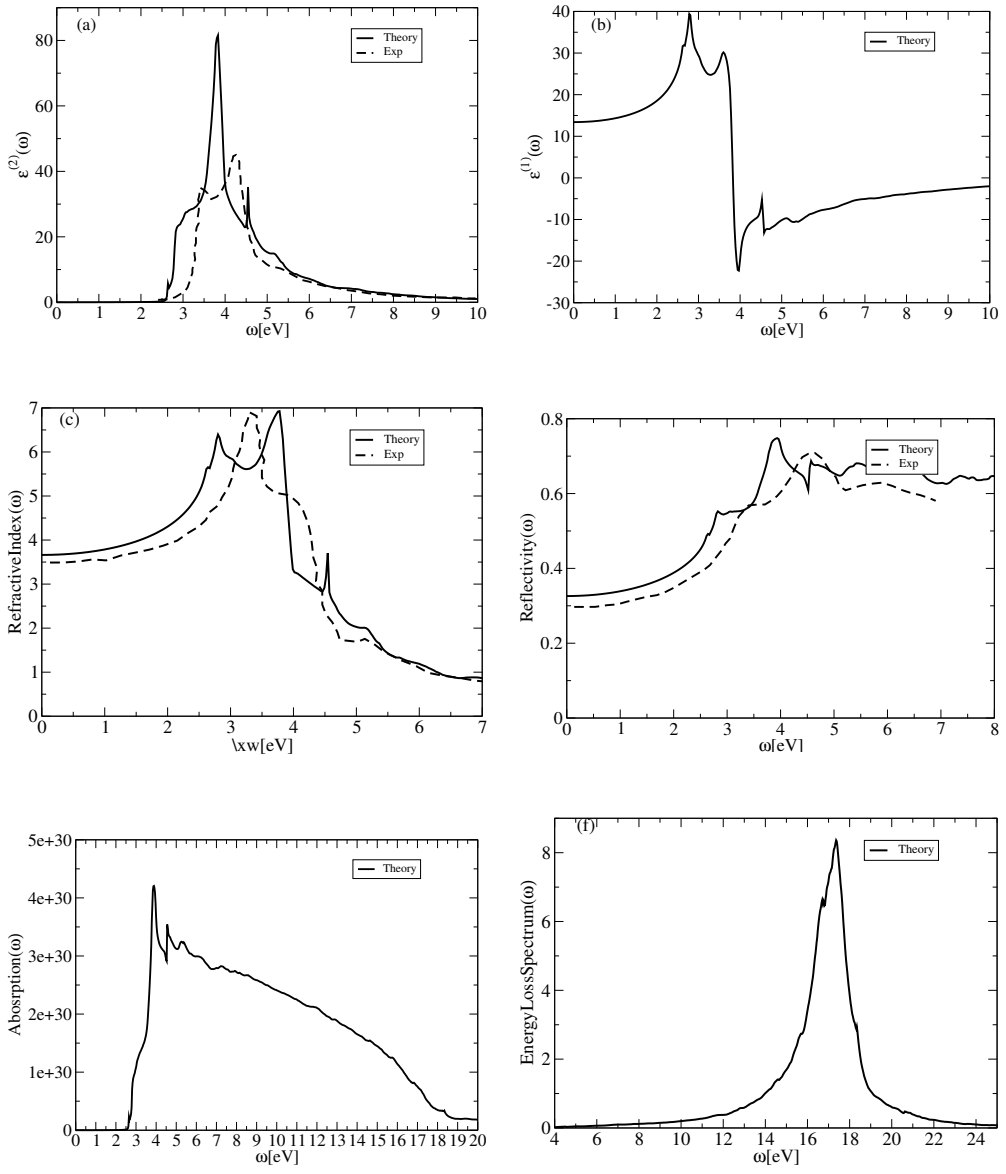

Figure 4.11: Calculated imaginary, real dielectric functions, refractivecoefficient, reflectivity, absorption and EnergylossSpectrum for 3C Si

Diamond Optical plots

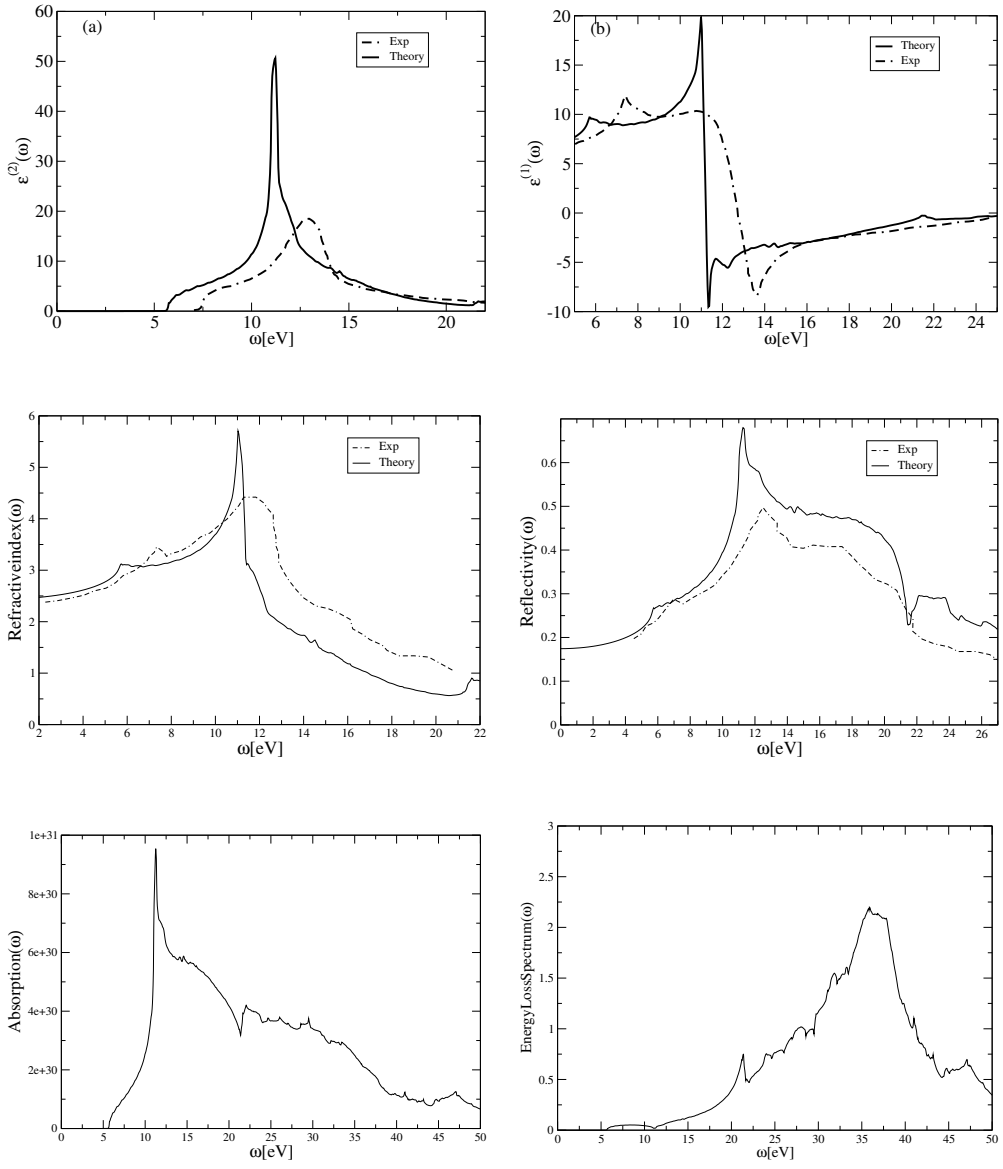

Figure 4.12: Calculated imaginary, real dielectric functions, refractivecoefficient, reflectivity, absorption and EnergylossSpectrum for 3C diamond

InAs Optical plots

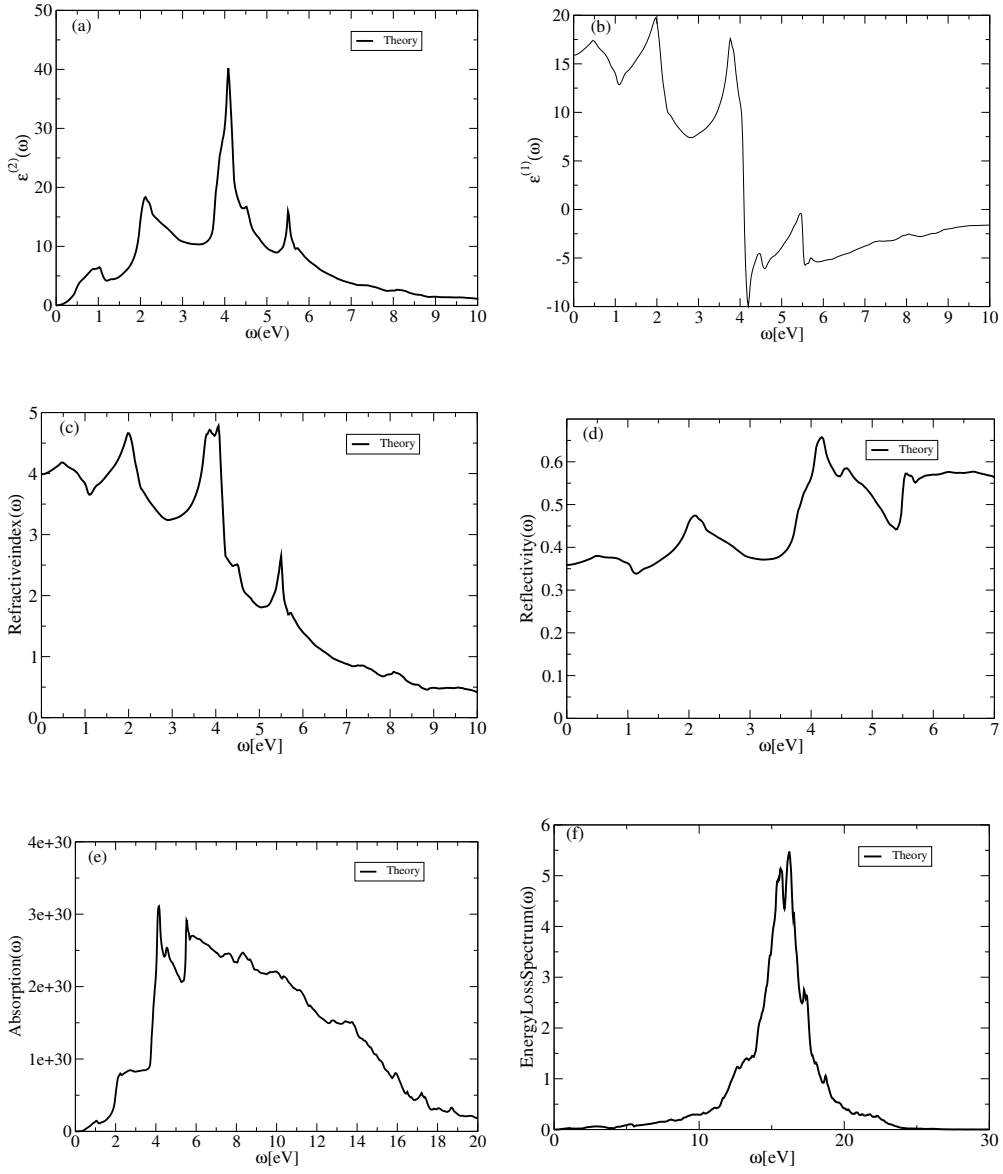

Figure 4.13: Calculated imaginary, real dielectric functions, refractivecoefficient, reflectivity, absorption and EnergylossSpectrum for 3C InAs

ZnO Optical plots

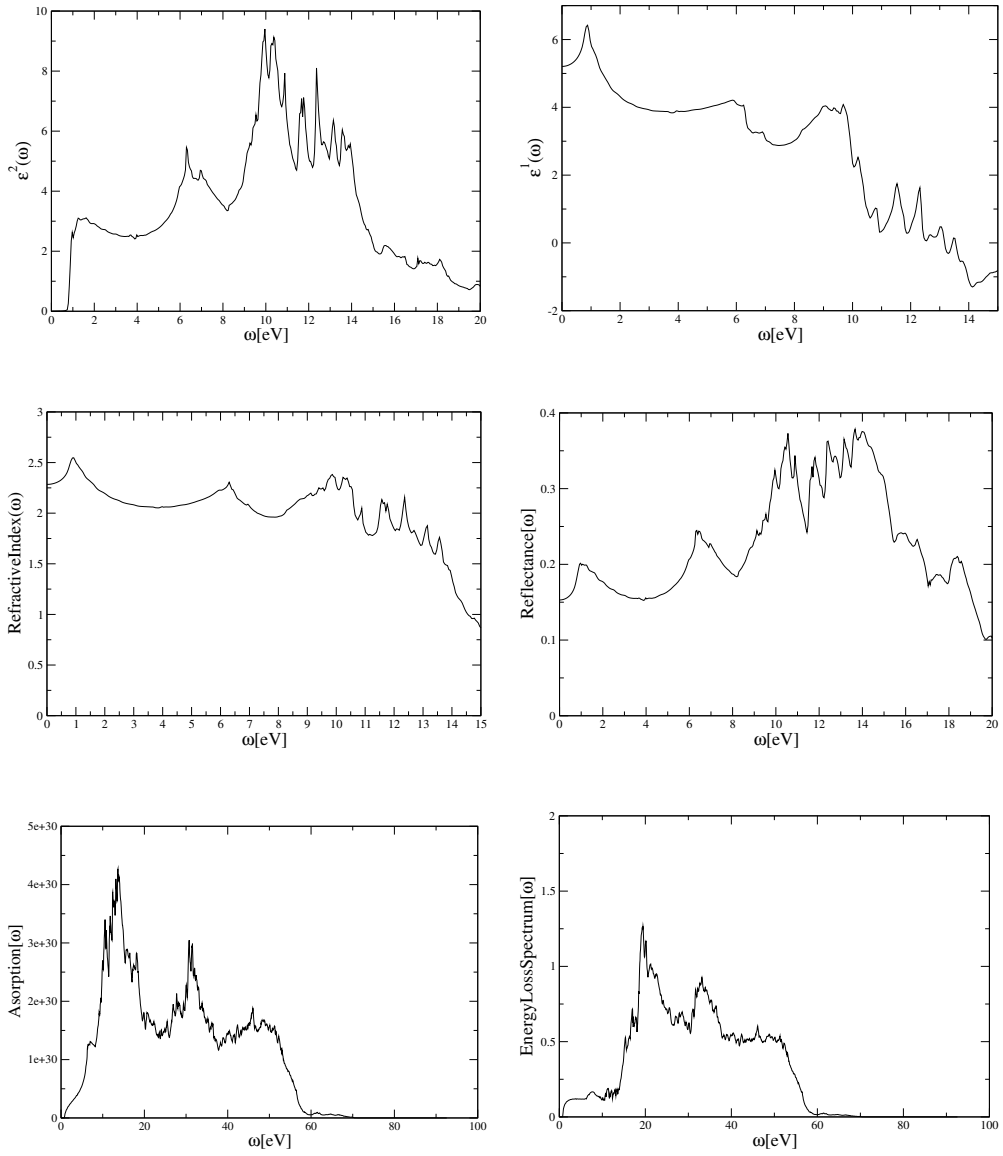

Figure 4.14: Calculated imaginary, real dielectric functions, refractivecoefficient, reflectivity, absorption and EnergylossSpectrum for wurzite ZnO

NiO Optical plots

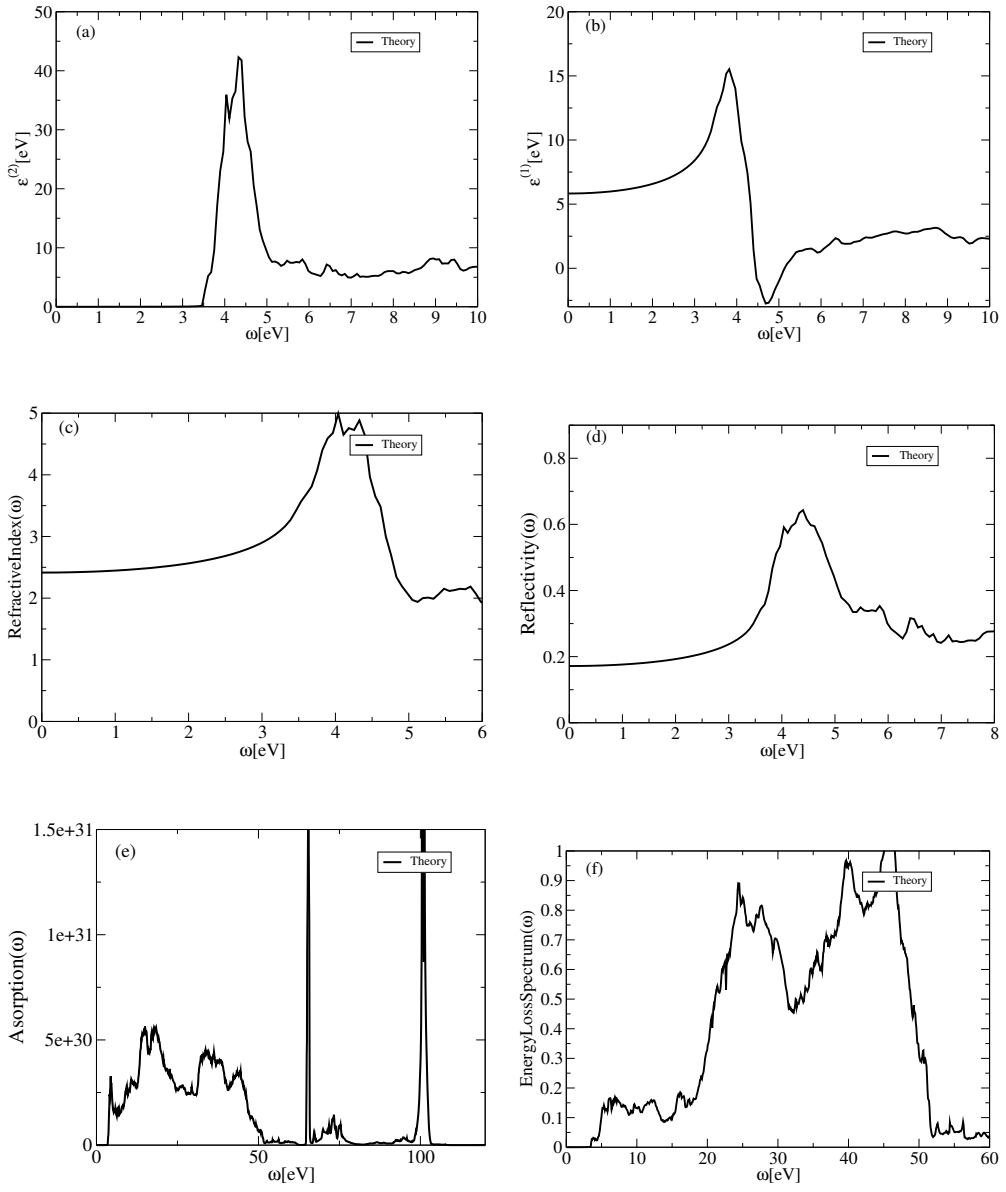

Figure 4.15: Calculated imaginary, real dielectric functions, refractivecoefficient, reflectivity, absorption and EnergylossSpectrum for FCC NiO

4.3.2 Static dielectric function

By using formula[2.38] the ion clamped static microscopic dielectric function in chapter in section. The dielectric constants were calculated using density perturbation theory within the PBE and PAW methodology was applied. In this static dielectric function calculations we used three different effects within longitudinal expression. In first effect, we omitted the local filed effects, ε_{mic}. In second effect, we considered the local field effects,ε_{RPA}. In third effect we considered the local filed effect including the Hartree approximation within the DFT level and represented as,ε_{DFT}. The 25x25x25 Monkhorst-Pack grid were applied and tetrahedron smearing method applied on Brillouin zone. The static values of different materials were shown in table[4.3].Theoretical calculations obtained from the effects are comparable with existing experimental data. The RPA method which used local effects showing accurate results when compared with other effects.

Symbol	Crsytal Structure	ε_{mic}^{LR}	ε_{RPA}^{LR}	ε_{DFT}^{LR}	Experiment
Si	Zincblende	13.511	12.130	12.905	11.7
GaAs	Zincblende	13.597	12.221	13.037	13.13
GaSb	Zincblende	18.267	16.587	17.650	
SiC	Zincblende	7.182	6.941	6.554	6.52
ZnO	Wurzite	5.843	5.479	5.516	
GaN	Wurzite	6.102	5.955	5.611	
ZnS	Zincblende	6.325	5.926	5.6	
C	Diamond	5.960	5.525	5.826	5.5
BN	Zincblende	4.703	4.351	4.601	
MgO	Rock salt	3.868	3.632	3.801	
LiF	Rock salt	2.047	1.930	2.020	
AlAs	Zincblende	9.830	8.569	9.271	10.1
AlN	Zincblende	4.709	4.560	4.560	
AlP	Zincblende	8.738	7.517	8.086	7.54
AlSb	Zincblende	12.090	10.656	11.522	10.3
InAs	Zincblende	18.767	17.315	18.190	14.55
AlP	Zincblende	11.030	9.820	10.485	
AlSb	Zincblende	12.261	11.125	11.803	10.3

Table 4.3: The static dielectric constants for the materils where shown for different local field effects

Chapter 5

Conclusions

In this thesis, ab initio calculations have been performed to study the (i) optical properties and (ii) effects of hybrid functionals on electronic structure and magnetic properties of selected materials. The band-gaps obtained from hybrid functionals were in good agreement with the experimental results except for ZnO, NiO, EuO and GdN. The results obtained from PBE+U of NiO, EuO and GdN bulk materials were comparable with previous theoretical works. NiO was stable in AFM II nature in HSE calculations, in agreement with experiments. The HSE06 method was unable to open a band gap in EuO. The spin up and spin down f electron bands of Eu couldn't be shifted from the Fermi level. In HSE06 calculation GdN showed semi-metalic nature. The dynamic dielectric functions were calculated and most of them were in good agreement with previous theoretical calculations and experimental results, wherever available. Also, the static dielectric constants were evaluated and were compared with other theoretical results.

Appendix i

FORTRAN PROGRAM TO CALCULATE DIFFERENT OPTICAL FUNCTIONS

```
program exp
implicit none
integer nmax1,countu,N,I,IO,nmax
real c,h
parameter(c=2.99792E10)
parameter(h=4.13566733E-15)
real,allocatable,dimension(:) :: Eev,x,y,z,xy,yz,zx,eimg,ereal,Eevr,xr,yr
real,allocatable,dimension(:) :: zr,xyr,yzr,zxr,abor,freq,refractive,energylossspectrum,
extinction,reflectivity
countu=0
OPEN(1,FILE = 'no.dat')
READ(1,*) nmax1
nmax=nmax1-1
allocate(Eev(nmax))
allocate(x(nmax))
allocate(y(nmax))
allocate(z(nmax))
allocate(xy(nmax))
allocate(yz(nmax))
allocate(zx(nmax))
allocate(Eevr(nmax))
allocate(xr(nmax))
allocate(yr(nmax))
allocate(zr(nmax))
allocate(xyr(nmax))
allocate(yzr(nmax))
allocate(zxr(nmax))
allocate(eimg(nmax))
allocate(ereal(nmax))
allocate(abor(nmax))
allocate(freq(nmax))
allocate(refractive(nmax))
allocate(energylossspectrum(nmax))
allocate(extinction(nmax))
allocate(reflectivity(nmax))
OPEN(2,FILE = 'img.dat',STATUS='OLD')
OPEN(3,FILE = 'rel.dat',STATUS='OLD')
```

```
OPEN(4,FILE = 'abor.dat')
OPEN(5,FILE = 'refractivecoefficient.dat')
OPEN(6,FILE = 'energylossspectrum.dat')
OPEN(7,FILE = 'extinction.dat')
OPEN(8,FILE = 'reflectivity.dat')
!read the number of points

    do 10 i=1,nmax
READ(2,*) Eev(i),x(i),y(i),z(i),xy(i),yz(i),zx(i)
countu=countu+1
10 end do
do 30 i=1,nmax
eimg(i)=(x(i)+y(i)+z(i))/3
30 end do
do 20 i=1,nmax
READ(3,*) Eevr(i),xr(i),yr(i),zr(i),xyr(i),yzr(i),zxr(i)
countu=countu+1
20 end do
do 40 i=1,nmax
ereal(i)=(xr(i)+yr(i)+zr(i))/3
freq(i)=(Eevr(i)*1.4142)/h
40 end do
do 50 i=1,nmax
abor(i)=1.4142*(freq(i)/h)*(SQRT(-ereal(i)+SQRT(eimg(i)*eimg(i)+ereal(i)*ereal(i))))
50 end do
do 60 i=1,nmax
refractive(i)=(SQRT(ereal(i)+SQRT(eimg(i)*eimg(i)+ereal(i)*ereal(i))))/1.4142
60 end do
do 70 i=1,nmax
energylossspectrum(i)=eimg(i)/(eimg(i)*eimg(i)+ereal(i)*ereal(i))
70 end do
do 80 i=1,nmax
extinction(i)=(SQRT(-ereal(i)+SQRT(eimg(i)*eimg(i)+ereal(i)*ereal(i))))/1.4142
80 end do
do 90 i=1,nmax
reflectivity(i)=((refractive(i)-1)*(refractive(i)-1)+extinction(i)*extinction(i))/ !
((refractive(i)+1)*(refractive(i)+1)+extinction(i)*extinction(i))
90 end do

    ! write(*,*) c ,h
do 500 i=1,nmax
```

```
write(4,*) Eev(i),abor(i)
500 end do
do 510 i=1,nmax
write(5,*) Eev(i),refractive(i)
510 end do
do 520 i=1,nmax
write(6,*) Eev(i),energylossspectrum(i)
520 end do
do 530 i=1,nmax
write(7,*) Eev(i),extinction(i)
530 end do
do 540 i=1,nmax
write(8,*) Eev(i),reflectivity(i)
540 end do
deallocate(Eev)
deallocate(x)
deallocate(y)
deallocate(z)
deallocate(xy)
deallocate(yz)
deallocate(zx)
deallocate(Eevr)
deallocate(xr)
deallocate(yr)
deallocate(zr)
deallocate(xyr)
deallocate(yzr)
deallocate(zxr)
deallocate(eimg)
deallocate(ereal)
deallocate(abor)
deallocate(freq)
deallocate(refractive)
deallocate(energylossspectrum)
deallocate(extinction)
deallocate(reflectivity)
CLOSE(2)
CLOSE(3)
CLOSE(4)
CLOSE(5)
CLOSE(6)
```

```
CLOSE(7)
CLOSE(8)
end program exp
```

Acknowledgements

I wish thank my supervisor Biplab Sanyal for his supervision and guidance. Biplab Sanyal , who first led me to enter the field of computational material science and provided good support and information. Your encouragement and motivation have created confidence in me to complete this task successfully. Special thanks for clarifying doubts which i asked repeatedly.

Thanks to Lars Nordstrom for reviewing my report and he also gives me useful suggestions to improve written skills.

I thank Satadeep Bhattacharjee for providing information about f electron systems and answering to my questions. I have discussed science and shared happy moments with: Biswarup Pathak , Kartick Tarafder, Sumanta Bhandary, Muhammed Ramzan, Jawad Nisar, Thanayut Kaewmaraya, Tanveer Hussain.

I would like thank to my friends, Madhu, Chetan, Ravi, Kiran Kovi, Raju, Kiran, Chandu, Naveen, Harisha, Sri.

Bibliography

[1] M. Born and R. Oppenheimer.Ann. Phys. **84** (20), 457 (1927).

[2] Hohenberg Pierre Walter Kohn (1964), Physical Review **136** (3B): B864B871.

[3] Vlastimil Mikolasa Mojmir Tomasekb (1977), Physics Letters A **64** Pages 109-110

[4] W. Kohn and L. J. Sham, Phys. Rev **140**, A1133 (1965).

[5] D. C. Langreth and J. P. Perdew, Phys. Rev. B **21**, 5469 (1980).

[6] D. C. Langreth and M. J. Mehl, Phys. Rev. B **28**, 1809 (1983).

[7] J. P. Perdew and Y. Wang,Phys. Rev. B **33**, 8800 (1986).

[8] J. P. Perdew ,Phys. Rev. B **33**, 8822 (1986).

[9] R.Resta ,Phys. Rev. B **27**, 36203630 (1983).

[10] S. L. Adler, Phys. Rev. **126**, 413 (1962)

[11] N. Wiser, Phys. Rev. **129**, 72 (1963)

[12] M. Gajdo, K. Hummer, G. Kresse, J. Furthmller, and F. Bechstedt,Phys. Rev. B **73**, 045112 (2006).

[13] P. Hohenberg and W. Kohn,Phys. Rev. **136**, B864 (1964).

[14] P. A. M. Dirac Proc. Royal Soc. (London) A,**123**, 714, (1929).

[15] J. P. Perdew and Alex Zunger.Phys. Rev. B **23**(10), 5048 (May 1981).

[16] D. M. Ceperley and B. J. Alder.Phys. Rev. Lett. **45**(7), 566 (August 1980).

[17] "www.scm.com/Doc/thesis.leeuwen.pdf"

[18] G Kresse and J Furthmuller Computational Materials Sceinces **6**(1) (1996)

[19] P. E. Blöchl, Physical Review B **50**, 17953 (1994)

[20] P. Perdew, M. Ernzerhof, and K. Burke, J. Chem. Phys.**105**, 9982 (1996).

[21] "python.rice.edu/~guscus/preprints/J_Heyd_Thesis.pdf"

[22] Aliaksandr ,V. Krukau, Oleg A. Vydrov, Artur F. Izmaylov, and Gustavo E. Scuseria THE JOURNAL OF CHEMICAL PHYSICS **125**, 224106 (2006).

[23] Ming-Zhu, Huang and W. Y. Ching , Phys. Rev. B **47** ,9449-9463(1993).

[24] Toon-Suk kim ,Yoon-Suk Kim, Kerstin Hummer, and Georg Kresse, Phys. Rev. B **80** (2009), 035203.

[25] M.Gajdos,K.Hummer, and G.Kresse, Phys .Rev B **73**, 045112 2006

[26] R.M.Sternheimer Phys. Rev. **96**, 951 (1954).

[27] M. R. Oliver , Phys. Rev. Lett. **24**, 1064 (1970)
4 1 1, 7 1, 8 1, 8 1, 8 2 2 2 2 2 5 7 7 7 8 17 9, 17 8 10 10 10 10 12, 13 13